Med. J. Cairo Univ., Vol. 90, No. 6, September: 1703-1713, 2022
www.medicaljournalofcairouniversity.net

The Role of Conventional Chest Imaging using Artificial Intelligence in COVID-19 Patients

RENAD MAGDY MOHAMMED, M.Sc.; SAHAR M. EL FIKY, M.D. and ASMAA M.M. SALAMA, M.D.

The Department of Radiodiagnosis, Faculty of Medicine, Ain Shams University

Abstract

Background: Diagnostic imaging is regarded as fundamental in the clinical work-up of patients with a suspected or confirmed COVID-19 infection. Recent progress has been made in diagnostic imaging with the integration of artificial intelligence (AI) and machine learning (ML) algorisms leading to an increase in the accuracy of exam interpretation and to the extraction of prognostic information useful in the decision-making process.

Aim of Study: To evaluate diagnostic accuracy of conventional radiography (CXR) using deep learning (DL) algorithms for the detection of pneumonia in COVID-19 patients and comparing findings with CT chest.

Subjects and Methods: This study was retrospective study conducted at Radiology Department, Ain Shams University from November 2020 till the end of the study.

Results: There was significant direct proportional between both grades of CT and AI score as *p*-value was (<0.05). The sensitivity was more in AI, while specificity was more in x-ray using CT consolidations as a reference to assess.

Conclusion: AI, applied to the interpretation of radiological images, allows to streamline and improve diagnosis while optimising the workflow of radiologists. Despite its low sensitivity compared to CT, efforts to improve the diagnostic yield of CXR are of the utmost interest, since it is the most common and widely used imaging method. Used as support in clinical practice and, in conjunction with other diagnostic techniques, it could help increase efficiency in the management of the COVID-19 infection.

Key Words: *Chest X-ray – Computed tomography – Covid-19 – Artificial intelligence – Deep learning.*

Introduction

AS the COVID-19 pandemic caused by SARS-CoV-2 spreads in the world, there is growing interest in the role and appropriateness of conventional chest radiographs (CXR) and computed tomography (CT) for management of patients with suspected or known COVID-19 infection. As the chest CT and CXR imaging pattern is non-specific and overlaps with other infections, the diagnostic value of imaging for COVID-19 is low and dependents upon radiographic interpretation. One study found that 56% of patients who presented within two days of diagnosis had a normal CT **[1]**. Conversely, other studies have identified chest CT abnormalities in patients prior to the detection of SARS-CoV-2 RNA. Given the variability in chest imaging findings, the American College of Radiology (ACR) does not recommend chest radiographs or CT alone for the diagnosis of or screening for COVID-19 **[2]**. Generally, the findings on chest imaging in COVID-19 are non-specific and overlap with other infections, including influenza, H1N1, severe acute respiratory syndrome (SARS) and Middle East respiratory syndrome (MERS) **[3,4]**. Therefore, detection of SARS-CoV-2 RNA is required, even if radiologic findings are suggestive of COVID-19 on CXR or CT **[2]**.

Conventional radiography, however, plays a role in the detection and follow-up of lung changes in patients with COVID-19, and CT should be reserved for hospitalized, symptomatic patients with specific clinical indications such as the investigation for pulmonary embolism or other complications **[1]**.

The recent medical applications of deep learning (DL) algorithms have been attracting increasing attention. In particular, the performances of DL algorithms have attracted attention for the detection of pulmonary malignancy, active tuberculosis, pneumothorax, and pneumonia in CXR images **[5-9]**. Previous research has demonstrated the clinical efficacy of the DL algorithm in terms of its ability to improve speed and accuracy in image reading **[7,10]**. If the DL algorithm achieves a performance that is equivalent to that achieved by physicians in the detection of radiological changes in CXR

Correspondence to: Dr. Renad M. Mohammed,
E-Mail: renadamin2006@yahoo.com

with COVID-19 pneumonia, the automatic interpretation of the CXR with DL algorithms can significantly reduce the burden on clinicians and radiologists in a sudden surge of suspected COVID-19 patients. The aim of this study was to evaluate the efficacy of DL algorithms for detecting COVID-19 pneumonia on CXR compared with radiological reports.

This study demonstrates the automatic interpretation of the CXR in detecting consolidation, which is a major finding that indicates pneumonia in corona virus patients [11].

In this retrospective analysis of CXR images and CT images in COVID-19 patients, our goal is to compare the detection performance of human radiologist and Artificial intelligence (AI), to see if AI would be capable of detecting at human expert-level or more, correctly finding lesions from a chest X-ray of a corona virus infected patient and comparing it to CT findings.

Patients and Methods

This was a retrospective study which conducted at Ain Shams University Hospitals from November 2020 to May 2021. The study was performed on convenient sample consists of 33 patients done during the study period at the Ain Shams hospital and meeting the study inclusion criteria. An acceptance from the ethical committee of the Radiology Department and The Ethical Committee of Faculty of Medicine, Ain Shams University was obtained to use the data stared on PACS system with the patients consent waived being a retrospective study. The privacy of participants and confidentiality of data was guaranteed during the various phases of the study.

Inclusion criteria:

- Known COVID-19 patients with positive PCR test.
- Patients having chest symptoms with no age predilection.
- Patients underwent both CXR and CT chest, within short period (less than one week).

Exclusion criteria:

- Patients with contraindication to radiation as pregnant females.
- Patients with chest symptoms having PCR negative test.
- Patients underwent both CXR and CT chest within period more than one week.

Method of CXR examination:

Patient's preparation: No specific preparation needed and no fasting was required. Positioning: in poster anterior projection or anteroposterior projection by different ranges of both KV and MA/S according to the age and weight of the patient especially if a child.

Method of HRCT examination:

Patient’s preparation: No specific preparation needed and no fasting was required. The patients were asked to lie supine on the CT table and asked to hold their breathing as long as they can until the end of the study to avoid breathing motion artifacts.

Fundamental technical protocols:

Slice thickness: 5-1.25mm, scan time: 0.5-1 second, KV: 120, mAs: 250, collimation: 1.5-3mm, matrix size: 768 x 768 or the largest available, FOV: 40cm, reconstruction algorithm: high spatial frequency, window: Lung window, patient position: Supine (routinely) and level of inspiration: Full inspiration (routinely recommended).

Image interpretation:

The study demonstrates the automatic interpretation of the CXR with Lunit INSIGHT software that can assist radiologists in the interpretation of CXR. The software, Lunit INSIGHT CXR, can discover multiple radiologic findings including lung consolidation, which indicates possible coronavirus (COVID-19) infected pneumonia. Analyses were performed using the picture archiving and communication system (PACS) of our hospital. We will assess the images of CXR of known COVID-19 patients having chest symptoms for the presence of lung consolidation (yes/no) and disease extent (i.e., percentage of affected lung parenchyma) [(I) <25%, (II) 25-50%, (III) >50-75%, (IV) >75%] of pneumonia in the conventional images. Radiologists read the films and are blinded to the results of AI and CT chest.

The Lunit Insight software interprets the images of CXR for the presence of consolidation and its percentage of affected lung parenchyma. Results are recorded in order to be compared by the results from human radiologists in both CXR and CT chest findings. CTs (which served as standard of reference) were read using the same classifications as for conventional radiography (presence (yes/no) and disease extent (I-IV). Additionally, the reader had to state the type of lung changes present on CT i.e., classic consolidation versus Ground glass opacities (GGOs). If both, classic consolidation and GGOs, were present the reader had to state that both types were present. The reader was aware of patients' symptoms but blinded to CXR and AI diagnosis.

Data management and analysis:

The collected data was revised, coded, tabulated and introduced to a PC using Statistical package for Social Science (SPSS 23). Data was presented and suitable analysis was done according to the type of data obtained for each parameter. Mean, Standard deviation (± SD) and range for parametric numerical data, while Median and Interquartile range (IQR) for non-parametric numerical data. Frequency and percentage of non-numerical data. p-value: Level of significance: -p>0.05: Non significant (NS), p<0.05: Significant (S).

Results

Table (1): Demographic data for the study group.

	N/Mean	%/SD	Median (IQR)	Range
Sex:				
Male	19	57.6%		
Female	14	42.4%		
Age	44.12	29.67	55 (9-70)	(0.5-86)

This study was conducted on 33 patients, 57.6% were males and 42.4% were females with mean age of the study group was 44.12±29.67 years ranged from 0.5 to 86 years.

Table (2): X-Ray findings for the study group.

			N	%
Left lung on X-ray	Consolidation	No	11	33.3
		Yes	22	66.7
Right lung on X-ray	Consolidation	No	11	33.3
		Yes	22	66.7
	Laterality	No	7	21.2
		Unilateral	8	24.2
		Bilateral	18	54.5
	Grade	No	7	21.2
		I	6	18.2
		II	6	18.2
		III	7	21.2
		IV	7	21.2

Regarding X-ray findings, 66.7% of patients had consolidations on left and right lungs. 54.5% had had bilateral consolidations while 24.2% had unilateral consolidations. Most of patients had grade III & IV by 21.2% and grade I & II by 18.2% for each group.

Table (3): Artificial intelligence findings for the study group.

	N/ Mean	%/ SD	Median (IQR)	Range
Left lung on AI:				
Consolidation:				
No	9	27.3%		
Yes	24	72.7%		
Right lung on AI:				
Consolidation:				
No	6	18.2%		
Yes	27	81.8%		
Score of AI	72%	32%	90% (56%-98%)	(0%-99%)

Regarding AI findings, 72.7% of patients had consolidations on left lung and 81.8% on right lung. Mean score of AI was 72%±32% ranged from 0% to 99%.

Table (4): Chest CT findings for the study group.

		N	%
Left lung on AI:			
Consolidation:	No	8	24.2
	Yes	25	75.8
GGO	No	8	24.2
	Yes	25	75.8
Both	No	13	39.4
	Yes	20	60.6
Lobes	No	3	9.1
	Upper	1	3.0
	Lower	13	39.4
	All	16	48.5
Right lung on CT:			
Consolidation:	No	4	12.1
	Yes	29	87.9
GGO	No	7	21.2
	Yes	26	78.8
Both	No	10	30.3
	Yes	23	69.7
Lobes	No	1	3.0
	Lower	6	18.2
	All	18	54.5
	Two lobes	8	24.2
Laterality	No	2	6.1
	Unilateral	2	6.1
	Bilateral	29	87.9
Grade	No	1	3.0
	I	5	15.2
	II	8	24.2
	III	8	24.2
	IV	11	33.3
Probability	Low	6	18.2
	Intermediate	4	12.1
	High	23	69.7
CORADS	1	1	3.0
	2	7	21.2
	3	2	6.1
	4	6	18.2
	5	17	51.5
Effusion	No	21	63.6
	Yes	12	36.4

Regarding CT findings, 75.8% of patients had consolidations on left lung and 87.9% on right lungs. 87.9% had had bilateral consolidations while 6.1% had unilateral consolidations. Most of patients had grade IV by 33.3%, grade II & III by 24.2% and grade I by 15.2%. 69.7% of patients had high probability while 18.2% and 12.1 had low and intermediate probabilities respectively.

Most patients had CORADS score 5 by 51.5%, grade 2 by 21.2% and 18.2%, 6.1% & 3% CO-RADS scores 4, 3 & 1 respectively. 36.4% of the study group had effusion.

Table (5): Relation between Age and Grades of X-ray & CT.

	Age		One Way ANOVA	
	N	Mean ± SD	*p*-value	Sig.
Grade X-ray:				
No	7	28.14±30.9	0.047(AI)	S
I	6	30±25		
II	6	36.33±39.9		
III	7	56.14±19.58		
IV	7	66.86±13.37		
Grade CT:				
No	1	70	0.06	NS
I	5	37.8±37.33		
II	8	29±28.3		
III	8	33.75±30.54		
IV	11	63.18±17.03		

(A) One Way ANOVA test of significance.
*Post-hoc test was significant between: (A1) between Grade 4 Vs. (grade 0 and grade 1).

Regarding relation between age and grades of X-ray and CT, there was significant difference between grades of X-ray as *p*-value was (<0.05) post hoc test was done to determine the significance between which groups and it was between grade 4 Vs. grades 0 and 1. There was no significant difference between grades of CT as *p*-value was (>0.05).

Table (6): Correlation between age and AI score.

Age	AI Score
Pearson correlation (*r*)	0.508
p-value	0.003
Sig.	S

Correlation was done to assess the relation between age and AI score, there was moderate positive correlation with significant *p*-value as it was (<0.05).

The relation between grades of X-ray and grades of CT, there was significant difference between both grades as *p*-value was (<0.05). The most correlated grades was grade IV, 100% of patients had grade IV by X-ray also had grade IV by CT.

The relation between grades of CT and AI score, there was significant direct proportional between both grades of CT and AI score as *p*-value was (<0.05).

Table (7): Relation between grade of CT and grade of X-ray.

	Grade CT					Fisher's exact test	
	No	I	II	III	IV		
	N (%)	N (%)	N (%)	N (%)	N (%)	*p*-value	Sig.
Grade X-ray:							
No (N=7)	1 (14.3%)	3 (42.8%)	2 (28.6%)	0 (0%)	1 (14.3%)	0.001	S
I (N=6)	0 (0%)	0 (0%)	3 (50%)	3 (50%)	0 (0%)		
II (N=6)	0 (0%)	1 (16.7%)	2 (33.3%)	3 (50%)	0 (0%)		
III (N=7)	0 (0%)	1 (14.3%)	1 (14.3%)	2 (28.6%)	3 (42.8%)		
IV (N=7)	0 (0%)	0 (0%)	0 (0%)	0 (0%)	7 (100%)		

Table (8): Relation between grade of CT and Score of AI.

	Grade CT					One way ANOVA	
	No (N=1)	I (N=5)	II (N=8)	III (N=8)	IV (N=11)		
	Mean ± SD	Mean ± SD	Mean ± SD	Mean ± SD	Mean ± SD	*p*-value	Sig.
Score AI	30%	42.6%±37.39%	58.75%±36.35%	74.63%±24.37%	97.55%±2.62%	0.002	S

We compared the sensitivity and specificity of X-ray and AI consolidations on left lung using CT consolidations as a reference to assess its predictive role to use it instead of CT, the sensitivity was more in AI, while specificity was more in than x-ray with significant difference in both X-ray and AI as *p*-value was (<0.05). AUC for X-ray and AI was 0.858 & 0.815 respectively.

The sensitivity and specificity of X-ray and AI consolidations on right lung using CT consolidations as a reference, the sensitivity was more in AI, while specificity was more in than X-ray with significant difference in both X-ray and AI as *p*-value was (<0.05). AUC for X-ray and AI was 0.879 & 0.823 respectively.

Clinical picture:

A 15 year old young boy, known case of acute myloid leukemia presented to the ER with high grade fever, cough and blood tinged sputum.

Table (9): Correlation between left lung consolidation on X-ray & AI using left lung consolidation on CT as a reference.

Left lung consolidation	CT		AUC	*p*-value	Sensitivity	Specificity	PPV	NPV
	Yes (N=25)	No (N=8)						
X-ray:								
Yes	21 (16%)	1 (12.5%)	0.858	<0.001	84%	87.50%	95.45%	63.64%
No	4 (16%)	7 (87.5%)						
AI:								
Yes	22 (88%)	2 (25%)	0.815	<0.001	88%	75%	91.7%	66.7%
No	3 (12%)	6 (75%)						

Table (10): Correlation between right lung consolidation on X-ray & AI using right lung consolidation on CT as a reference.

Right lung consolidation	CT		AUC	*p*-value	Sensitivity	Specificity	PPV	NPV
	Yes (N=29)	No (N=4)						
X-ray:								
Yes	22 (75.9%)	0 (0%)	0.879	<0.001	75.86%	100%	100%	36.36%
No	7 (24.1%)	4 (100%)						
AI:								
Yes	26 (89.7%)	1 (25%)	0.823	0.012	89.66%	75%	96.30%	50.0%
No	3 (10.3%)	3 (75%)						

X-ray & AI findings:

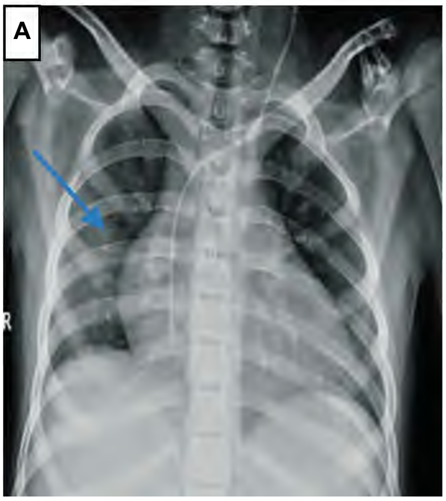

(A): CXR revealed right lung mid zone opacity (arrowed) with grade I severity.

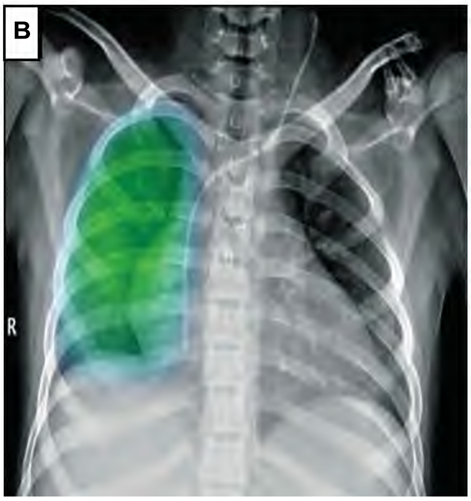

(B): DL algorithm heatmap overlaid on the image feature related to pneumonia in all zones of the right lung with score 56%.

Chest computed tomography:

(C,D,E): CT images showing right lung consolidation and ground-glass opacities. The patient was considered grade III severity with indeterminate probability of COVID-19 (CORADS 3).

Representative case of positive PCR COVID-19, which was suitably localized and detected by the DL algorithm. In this case the deep learning (DL) algorithm analysis of the localization of COVID-19 with pneumonia was similar with the findings in CT, better than conventional radiography.

Clinical picture:

A 42 year old female patient presented to the ER with dyspnea, tachypnea and decreased air entry on the right side.

X-ray & AI findings:

(A): CXR of patient with COVID-19 shows opacity in all zones of the right lung and left lung mid and lower zones denoting consolidation, with severity grade IV.

(B): DL algorithm classified CXR with probability score about 97%. the color map reveals affection of all zones of the right lung and left mid and lower zones as in conventional imaging.

Chest computed tomography:

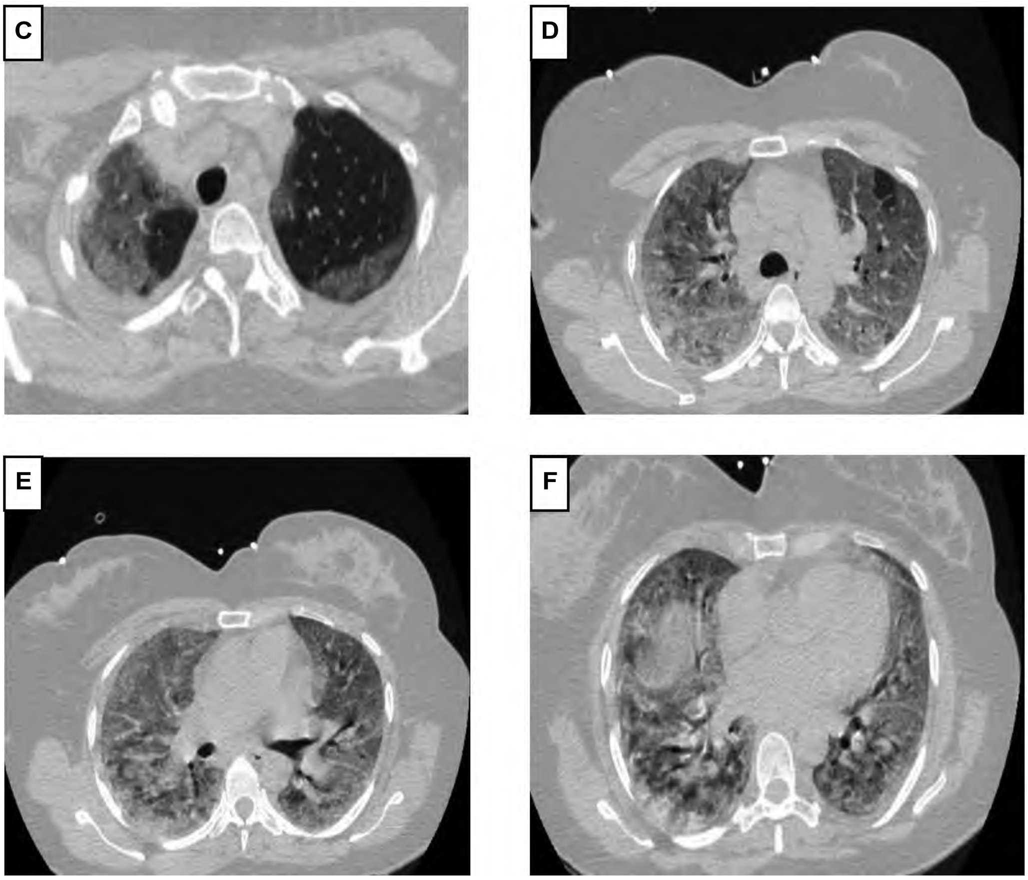

(C,D,E,F): CT images show diffuse bilateral asymmetrical coalescent opacities, also often demonstrates an anteroposterior density gradient within the lung, with dense consolidation in the most dependent regions, merging into a background of widespread ground-glass attenuation. The patient was considered to be of grade IV severity.

This patient was PCR positive for COVID-19, this case represents true positive for AI & CXR. ARDS was considered to be a complication of COVID-19.

Discussion

Diagnostic imaging is regarded as fundamental in the clinical work-up of patients with a suspected or confirmed COVID-19 infection. Recent progress has been made in diagnostic imaging with the integration of artificial intelligence (AI) and deep learning (DL) algorisms leading to an increase in the accuracy of exam interpretation and to the extraction of prognostic information useful in the decisionmaking process. Considering the ever expanding imaging data generated amid this pandemic, COVID-19 has catalyzed the rapid expansion in the application of AI to combat disease **[12]**.

The aim of this study was to evaluate the diagnostic accuracy of conventional radiography (CXR) using deep learning (DL) algorithms for the detection of pneumonia in COVID-19 patients and comparing findings with CT chest.

This was a retrospective study, conducted at the radio diagnosis department of Ain Shams University hospitals, in the period from 3-6 months, the study was carried out on 33 patients with realtime polymerase chain reaction (RT-PCR) confirmed COVID-19 patients referred to Ain Shams University Radiology Unit underwent CXR and CT chest.

The study involved 33 patients, 57.6% were males and 42.4% were females with mean age of the study group was 44.12±29.67 years ranged from 0.5 to 86 years.

Similar to our study, a retrospective study of Yasin and Gouda **[13]** with the plain radiography done for 350 patients who tested positive for coronavirus by nasopharyngeal swap. Age of the patients ranged from 12 to 85 years old with mean age was 41.68±14.12 years. There were 261 males and 89 females with male to female distribution of 2.9:1.

The CXR scoring system provides a semi-quantitative tool to assess lung abnormalities and help clinicians stratify the disease risk. A score, ranging from 0 to 4, was given to each lung in our study according to the extent of lung involvement [14].

Regarding X-ray findings, 66.7% of patients had consolidations on left and right lungs. 54.5% had had bilateral consolidations while 24.2% had unilateral consolidations. Most of patients had grade of severity III & IV by 21.2% and grade I & II by 18.2% for each group.

Similar to our study, In Yasin, and Gouda [13] study,the chest X-ray consolidation opacities were the most common finding seen in 218 patients (81.3%), followed by reticular interstitial thickening seen in 107 patients (39.9%) and GGO seen in 87 patients (32.5%). Pulmonary nodules were found 25 patients (9.3%) and pleural effusion was seen in 20 patients (7.5%). Most of the patients showed bilateral lung affection (181 patients, 67.5%) with peripheral distribution (156 patients, 58.2%) and lower zone affection (196 patients, 73.1%).

In concordance to our study, Sathi et al. [15] reported that in CXR the most common scores were mild (85.6%). Moderate severity scores were found in 13.5% of cases, while severe cases were found in 0.9% of cases. This was incorcordance to our study, as our study involves smaller number of cases that represented to the ER unit.

In recent years, medical diagnosis using AI-driven systems have demonstrated remarkable progress in assisting radiologists and clinicians for disease detection, characterization, and monitoring. The automated nature of AI to recognize intricate patterns in radiologic images and its ability to provide quantitative assessment offer an efficient and scalable mechanism to augment the current diagnostic workflow in the hospitals and ambulatory testing centers. There were preliminary works that utilized AIdriven methodologies to assist radiographic examinations in identifying the visual indicators highly associated with COVID-19 [16].

In the current study, Regarding AI findings, 72.7% of patients had consolidations on left lung and 81.8% on right lung. Mean score of AI was 72%±32% ranged from 0% to 99%.

Previous studies of Apostolopoulos and Mpesiana [17]; Asif et al. [18] focused on the automatic classification of COVID-19 from CXR images, considering how useful it could be in emergency departments, urgent care, and resource-limited settings. Moreover, by matching CXR findings to clinical data prognostic models can be developed, to predict disease gravity, and stratify patients on the basis of their risk of developing severe disease and or complications.

Regarding CT findings, 60.6% of patients had both GGO and consolidation in left lung and 69.7% of patients had both GGO and consolidation in right lung.75.8% of patients had consolidations on left lung and 87.9% on right lungs.78.8% had GGO in right lung and 75.8% had GGO in left lung. 87.9% had had bilateral lung affection while 6.1% had unilateral lung affection.

Furthermore, the study of Farghaly and Makboul [19] reported that there was no lung affection was observed at chest CT in 47 (8.2%), while 461 (80.3%) patients had bilateral lung affection and only 66 (11.5%) patients had unilateral affection.

Regarding lobar affection in CT, we found that 48.5% of cases had affection of both lobes of left lung & 54.5% of cases had affection of all lobes of right lung. 24.2% of cases had affection of two lobes of right lung. Regarding one lobe affection, the lower lobe was the commonest lobe involved in both lungs (87.9% in left lung and 96.6% in right lung).

In comparison with our findings, the study of Bernheim et al. [20] reported 94 patients out of 121 (77.6%) had ground-glass opacities, consolidation, or both, 41 (34%) had only ground-glass opacities (with no consolidation) and two (2%) had consolidation in the absence of ground-glass opacities. Eighteen patients (15%) had opacities in one lobe, 14 (12%) had two affected lobes, 11 (9%) had three affected lobes, 18 (15%) had four affected lobes and 33 (27%) had disease affecting all five lobes. Seventy-three of the 121 patients (60%) had bilateral lung disease. Twenty patients (17%) had exclusively unilateral lung involvement, including 13 patients with only right lung involvement and seven with only left lung involvement.

Regarding severity score, most of patients had grade IV by 33.3%, grade II & III by 24.2% and grade I by 15.2%. 69.7% of patients had high probability while 18.2% and 12.1 had low and intermediate probabilities respectively. Most patients had CORADS score 5 by 51.5%. 36.4% of the study group had pleural effusion.

The study of Farghaly and Makboul [19] reported that CORADS-3 was presented in 442 (77%) patients, followed by COVID-RADS-0 in 47 (8.2%) patients, while CORADS-2 was presented in 85 patients (14.8%). Of the included patients, 156 (24.7%), 159 (27.7%), 136 (23.7%), and 76 (13.2%) patients had minimal, mild, moderate, and severe grades of affection respectively based on CT severity score.

Regarding relation between age and grades of X-ray and CT, we found that there was significant difference between grades of X-ray as *p*-value was (<0.05). There was no significant difference between grades of CT as *p*-value was (>0.05).

In our study, we assessed the relation between age and AI score, there was moderate positive correlation with significant *p*-value as it was (<0.05).

In a study of Borghesi et al. [21], 783 Italian patients (532 males and 251 females) with SARS-CoV-2 infection were enrolled. Similar to our study, a significant correlation was observed between the CXR score and age in both males and females. Males aged 50 years or older and females aged 80 years or older with coronavirus disease 2019 showed the highest CXR score.

Unlike to our study, Farghaly and Makboul [19] reported that regarding the relationship between age and severity of COVID-19, they found that there was a highly statistically significant difference between age and total CT severity lung score with (*p*-value <0.001), where young age (<30 year old) had the lowest total CT lung score, while the highest score was observed in old patients (≥70 years).

In our study, relation between grades of X-ray and grades of CT, there was significant difference between both grades as *p*-value was (<0.05). The most correlated grades was grade IV, 100% of patients had grade IV by X-ray also had grade IV by CT. Furthermore, the relation between grades of CT and AI score, there was significant direct proportional between both grades of CT and AI score as *p*-value was (<0.05).

In agreement with our findings, Çinkoog˘lu et al. [22] found a high positive correlation between total CTSs and XRSs (*rs*=0.70, *p*<0.001). Also, there were low to moderate positive correlations between CTSs and XRSs of each zone.

We compared the sensitivity and specificity of X-ray and AI consolidations on the lungs using CT consolidations as a reference to assess its predictive role to use it instead of CT, the sensitivity was more in AI, while specificity was more in X-ray with significant difference in both X-ray and AI as *p*-value was (<0.05). In left lung, AUC for X-ray and AI was 0.858 & 0.815 respectively. In right lung, AUC for X-ray and AI was 0.879 & 0.823 respectively.

A retrospective study of Li et al. [23] employed AI model that achieved AUC of 0.95 yielding higher accuracy (90%), sensitivity (88%), and specificity (91%) compared to manual interpretatin.

Hwang et al. [24] reported that for the identification of pneumonia with the reference standard of CT, AUC (0.789), sensitivity (74.0%), and specificity (72.4) of the radiologist in the CAD-assisted interpretation which did not significantly differ from those in the reader-alone interpretation.

The use of AI seeks to at least match the diagnostic performance of radiologists. Narin et al. [25] thus, demonstrated that the performance of an AI system to detect COVID-19 pneumonia was comparable to that of six independent radiologists, with an operating point of 85% sensitivity and 61% specificity in comparison to RT-PCR as the reference standard for the presence or absence of SARS-CoV-2 viral infection. The AI system correctly classified CXR images as COVID-19 pneumonia with an AUC of 0.81, significantly outperforming each reader (*p*<0.001) at their highest possible sensitivities.

Conclusion:

AI, applied to the interpretation of radiological images, allows to streamline and improve diagnosis while optimising the workflow of radiologists. Despite its low sensitivity compared to CT, efforts to improve the diagnostic yield of CXR are of the utmost interest, since it is the most common and widely used imaging method. Its use allows to monitor disease progression, provides an objective assessment based on quantitative information, reduces subjectivity and variability and allow the optimisation of resources due to its potential ability to predict the length of hospital stays. Used as support in clinical practice and, in conjunction with other diagnostic techniques, it could help increase efficiency in the management of the COVID-19 infection.

References

1- XU X., YU C., QU J., ZHANG L., JIANG S., HUANG D., CHEN B., ZHANG Z., GUAN W., LING Z., et al.: Imaging and clinical features of patients with 2019 novel coronavirus SARS-CoV-2. Eur. J. Nucl. Med. Mol. Imaging, 47: 1275-1280, 2020.

2- ACR Recommendations for the Use of Chest Radiography and Computed Tomography (CT) for Suspected COVID-19 Infection. [(accessed on 26 April 2020)]; Available online: https://www.acr.org/Advocacy-and-Economics/ACR-Position-Statements/Recommendations-for-Chest-Radiography-and-CT-for-Suspected-COVID19-Infection.

3- WANG Y., DONG C., HU Y., LI C., REN Q., ZHANG X., SHI H. and ZHOU M.: Temporal Changes of CT Findings in 90 Patients with COVID-19 Pneumonia: A Longitudinal Study. Radiology, 296: E55-E64, 2020.

4- ABBASI-OSHAGHI E., MIRZAEI F., FARAHANI F., KHODADADI I. and TAYEBINIA H.: Diagnosis and treatment of coronavirus disease 2019 (COVID-19): Laboratory, PCR, and chest CT imaging findings. Int. J. Surg., 79: 143-153, 2020.

5- GRAAT E.M., HENDRIKSE A.K., SPRONK P.E., KOREVAAR J.C., STOKER J. and SCHULTZ M.J.: Chest radiography practice in critically ill patients: A postal survey in the Netherlands. BMC Med. Imaging, 6: 8, 2006.

6- MARTINI K., BAESSLER M., BAUMUELLER S. and FRAUENFELDER T.: Diagnostic accuracy and added value of dual-energy subtraction radiography compared to standard conventional radiography using computed tomography as standard of reference. PLoS ONE, 12: e0174285, 2017.

7- HWANG E.J., PARK S., JIN K.N., KIM J.I., CHOI S.Y., LEE J.H., et al.: Development and Validation of a Deep Learning-Based Automated Detection Algorithm for Major Thoracic Diseases on Chest Radiographs. JAMA Netw Open, 2 (3): e191095, 2019.

8- LAKHANI P. and SUNDARAM B.: Deep learning at chest radiography: Automated classification of pulmonary tuberculosis by using convolutional neural networks. Radiology, 284 (2): 574-82, 2017.

9- NAM J.G., PARK S., HWANG E.J., LEE J.H., JIN K-N., LIM K.Y., et al.: Development and validation of deep learning-based automatic detection algorithm for malignant pulmonary nodules on chest radiographs. Radiology, 290 (1): 218-28, 2019.

10- KIM J.H., KIM J.Y., KIM G.H., KANG D., KIM I.J., SEO J., et al.: Clinical Validation of a Deep Learning Algorithm for Detection of Pneumonia on Chest Radiographs in Emergency Department Patients with Acute Febrile Respiratory Illness. Journal of Clinical Medicine, 9 (6), 2020.

11- How can AI help doctors fight corona virus?/https://www.lunit.io/en/covid19/

12- LAINO M.E., AMMIRABILE A., POSA A., CANCIAN P., SHALABY S., SAVEVSKI V. and NERI E.: The Applications of Artificial Intelligence in Chest Imaging of COVID-19 Patients: A Literature Review. Diagnostics, 11: 1317, 2021.

13- YASIN R. and GOUDA W.: Chest X-ray findings monitoring COVID-19 disease course and severity. Egypt J. Radiol. Nucl. Med., 51: 193, 2020.

14- ABOUGAZIA A., ALNUAIMI A., AMAL M., TAMER A., AHMED K., BANAN Q., AHMED S., SOUBHI Z., SERVET K., BARHAM A., YASSER A.Y., MOHAMED E., AHMED A. and REDA Y.: "Chest X-Ray Findings in COVID-19 Patients Presenting to Primary Care during the Peak of the First Wave of the Pandemic in Qatar: Their Association with Clinical and Laboratory Findings", Pulmonary Medicine, vol. 2021, Article ID 4496488, 8 pages, 2021.

15- SaTHI S., RICHA T., SAVITA V., ANIL K.G., VIRENDRA S.S., MANOJ K.S., AMIT M. and DEVINDER V.: "Role of Chest X-Ray in Coronavirus Disease and Correlation of Radiological Features with Clinical Outcomes in Indian Patients", Canadian Journal of Infectious Diseases and Medical Microbiology, Vol. 2021, Article ID 6326947, 8 pages 2021.

16- BALTAZAR L.R., MANZANILLO M.G., GAUDILLO J., VIRAY E.D., DOMINGO M., TIANGCO B., et al.: Artificial intelligence on COVID-19 pneumonia detection using chest xray images. PLoS ONE, 16 (10): e0257884, 2021.

17- APOSTOLOPOULOS I.D. and MPESIANA T.A.: Covid-19: Automatic Detection from X-Ray Images Utilizing Transfer Learning with Convolutional Neural Networks. Phys. Eng. Sci. Med., 43: 635-640, 2020.

18- ASIF S., WENHUI Y., JIN H., TAO Y. and JINHAI S.: Classification of COVID-19 from Chest X-Ray Images Using Deep Convolutional Neural Networks. In Proceedings of the 2020 IEEE 6th International Conference on Computer and Communications (ICCC), Chengdu, China, December, 11-14, 2020.

19- FARGHALY S. and MAKBOUL M.: Correlation between age, sex, and severity of Coronavirus disease-19 based on chest computed tomography severity scoring system. Egypt J. Radiol. Nucl. Med., 52, 23, 2021.

20- BERNHEIM X. MEI, HUANG M., YANG Y., FAYAD Z.A., ZHANG N., et al.: C.T. Chest Findings in coronavirus disease-19 (COVID-19): relationship to duration of infection, Radiology, 295: 200463, 2020.

21- BORGHESI A., ZIGLIANI A., MASCIULLO R., et al.: Radiographic severity index in COVID-19 pneumonia: Relationship to age and sex in 783 Italian patients. Radiol. Med., 125: 461-464, 2020.

22- ÇINKOOĞLU, A., BAYRAKTAROĞLU S., CEYLAN N., et al.: Efficacy of chest X-ray in the diagnosis of COVID-19 pneumonia: Comparison with computed tomography through a simplified scoring system designed for triage. Egypt J. Radiol. Nucl. Med., 52: 166, 2021.

23- LI L., QIN L., XU Z., YIN Y., WANG X., KONG B., BAI J., LU Y., FANG Z., SONG Q., et al.: Using Artificial Intelligence to Detect COVID-19 and Community-Acquired Pneumonia Based on Pulmonary CT: Evaluation of the Diagnostic Accuracy. Radiology, 296: E65-E71, 2020.

24- HWANG E.J., KIM K.B., KIM J.Y., LIM J-K., NAM J.G., CHOI H., et al.: COVID-19 pneumonia on chest X-rays: Performance of a deep learning-based computer-aided detection system. PLoS ONE, 16 (6): e0252440, 2021.

25- NARIN A., C. KAYA C. and Z. PAMUK L.: Automatic Detection of Coronavirus Disease (COVID-19) Using X-ray Images and Deep Convolutional Neural Networks. Pattern Analysis and Applications, 24 (3): 1207-20, 2021.

دور التصوير التقليدى للصدر باستخدام الذكاء الاصطناعى فى المرضى COVID-19

الخلفية : يعتبر التصوير التشخيصى أساسياً فى العمل السريرى للمرضى المصابين بعدوى بكوفيد-١٩ المشتبه بها أو المؤكد. تم إحراز تقدم مؤخراً فى التصوير التشخيصى من خلال دمج الذكاء الاصطناعى والتعلم الآلى مما أدى إلى زيادة دقة تفسير الامتحان واستخراج المعلومات الإنذارية المفيدة فى عملية صنع القرار.

الهدف من الدراسة : تقييم الدقة التشخيصية للتصوير الشعاعى التقليدى باستخدام خوارزميات التعلم العميق للكشف عن الالتهاب الرئوى لدى مرضى كوفيد-١٩ ومقارنة النتائج مع الصدر المقطعى المحوسب.

الموضوعات والطرق : أجريت هذه الدراسة بأثر رجعى فى قسم الأشعة بجامعة عين شمس من نوفمبر ٢٠٢٠ حتى نهاية الدراسة.

النتيجة : كان هناك تناسب مباشر معنوى بين درجتى التصوير المقطعى المحوسب ودرجة الذكاء الاصطناعى حيث كانت القيمة الاحتمالية (<٠.٠٥). كانت الحساسية أكثر فى الذكاء الاصطناعى، بينما كانت الخصوصية أكثر فى الأشعة السينية باستخدام التوحيد المقطعى كمرجع للتقييم.

الاستنتاج : يسمح الذكاء الاصطناعى ، المطبق على تفسير الصور الإشعاعية، بتبسيط التشخيص وتحسينه مع تحسين سير عمل أخصائى الأشعة. على الرغم من حساسيتها المنخفضة مقارنة بالتصوير المقطعى المحوسب، إلا أن الجهود المبذولة لتحسين العائد التشخيصى من إجراء أشعة سينية على الصدر تحظى باهتمام كبير، لأنها أكثر طرق التصوير شيوعاً والأكثر استخداماً. يستخدم كدعم فى الممارسة السريرية، وبالأقتران مع تقنيات التشخيص الأخرى، يمكن أن يساعد فى زيادة الكفاءة فى إدارة عدوى بكوفيد-١٩.